

# Aggregate and Firm-Level Stock Returns During Pandemics, in Real Time\*

Laura Alfaro<sup>†</sup>    Anusha Chari<sup>‡</sup>    Andrew Greenland<sup>§</sup>    Peter K. Schott<sup>¶</sup>

April 10, 2020

**Preliminary and Incomplete  
Comments Welcome!**  
Most recent version is [here](#)

## Abstract

We find that an unanticipated doubling of predicted infections during the COVID-19 and SARS pandemics forecast aggregate equity market value declines of 4 to 11 percent. We show that firm returns are sensitive to this information even after accounting for their co-movement with the overall market. Our results imply a decline in returns' reaction to new infections as the trajectory of the pandemic becomes clearer.

---

\*This paper is preliminary and incomplete. Missing citations and discussions of related research will be added in future drafts. We thank Nick Barberis, Lorenzo Caliendo, Teresa Fort, Mihai Ion, and Ed Kaplan for comments and suggestions. We thank Alex Schott and Mengru Wang for excellent research assistance.

<sup>†</sup>Harvard Business School & NBER (lalfaro@hbs.edu).

<sup>‡</sup>UNC Chapel Hill & NBER (achari@unc.edu).

<sup>§</sup>Martha and Spencer Love School of Business, Elon University (agreenland@elon.edu).

<sup>¶</sup>Yale School of Management & NBER (peter.schott@yale.edu).

# 1 Introduction

We show that unanticipated changes in predicted infections based on daily re-estimation of simple epidemiological models of infectious disease forecast stock returns during the SARS and COVID-19 pandemics. This relationship is consistent with investors using such models to update their beliefs about the economic severity of the outbreak, in real time, as they attempt to gauge risk in the face of uncertainty (Knight, 1921; Keynes, 1937).

We emphasize that we are *not* epidemiologists and are *not* outlining a method to characterize the true path of pandemics. We also are not trying to infer the efficacy of various intervention strategies.<sup>1</sup> Such efforts, while of immense value, require data which may not be available until after the outbreak is substantially underway. Rather, we view real-time changes in the predicted severity of an outbreak as potentially useful summary statistics of its ultimate consequences, especially before the true model is revealed.

We model cumulative infections as either exponential or logistic. We re-estimate the parameters of these models each day of the outbreak using information on reported cases up to that day (which arrives after trading closes on that day). We then use these parameters to compute the predicted number of cases for the next trading day  $t$  using the cumulative counts reported after closing on days  $t - 1$  and  $t - 2$ . The difference in these forecasts reflect unanticipated changes in the trajectory of the pandemic due to newly available information. We examine how these differences in projections covary with aggregate market returns on day  $t$ .

Applying this procedure to the United States during the current COVID-19 pandemic and to Hong Kong during the 2003 SARS outbreak, we find that sharper increases in predictions are associated with larger declines in market returns.<sup>2</sup> In the United States thus far, coefficient estimates imply declines of 4 to 10 percent in the Wilshire 5000 index in response to a doubling of predicted COVID-19 infections. We find a similar relationship during SARS, where a doubling of projected cases implies declines of 8 to 11 percent in the Hong Kong stock market’s Hang Seng index. These findings suggest equity markets become less responsive to new cases the more they adhere to *previously* estimated parameters.

We find that changes in forecasts retain their aggregate-market explanatory power even after controlling for a simpler summary of the severity of the outbreak, the most recent increase in reported cases. In contrast to this simple measure, estimated model parameters explicitly predict the eventual number of people that may be infected (e.g., the “carrying capacity” under the logistic model), and the speed with which that number may be reached. For example, a jump in estimated share of the population that ultimately will be infected suggests a larger labor supply shock, while an increase in the estimated growth rate of infections has implications for healthcare capacity constraints. We show that our results for the United States are robust to the inclusion of coarse controls for changes in federal and local policy.

Using disaggregate data, we find that individual firms’ returns are sensitive to unanticipated increases in predicted infections, and that this sensitivity persists even after accounting for their co-movement with the market (Sharpe, 1964a). While there is substantial heterogeneity in firm returns within sectors, average returns by sector vary in an intuitive way. Firms operating in industries more heavily affected by social distancing – Accommodations, Entertainment and Transportation – exhibit the greatest exposure to the pandemic and the largest declines in market value. Firms in Education, Professional Services and Finance, by contrast, are less sensitive, likely due to their

---

<sup>1</sup>Piguillem and Shi (2020) and Berger et al. (2020), by contrast, use estimates of micro-founded SEIR models to argue that expanded testing generates substantial welfare gains relative to quarantines.

<sup>2</sup>While our results at present focus on SARS in Hong Kong and COVID-19 in the United States, we are expanding the set of countries we analyze during the latter, and have begun a similar analysis for the 2009 H1N1 outbreak.

greater ability to continue operations online.

Our analysis contributes to several literatures. First, we add to the very large body of research on asset pricing that examines the predictability of stock returns. Seminal papers by [Campbell and Shiller \(1988\)](#), [Fama and French \(1988\)](#) and others show that factors ranging from valuation ratios to corporate payout and financing policies forecast stock returns. In this paper we draw upon standard epidemiological models to infer how investors might update their beliefs about disease progression.

Second, our examination of firm returns in response to changes in model predictions contributes to numerous studies in corporate finance, pioneered by [Ball and Brown \(1968\)](#) and [Fama et al. \(1969\)](#), which use plausible changes in investors’ information sets to understand market dynamics. In a typical event study, researchers examine specific events, such as an earnings announcements, that may release information relevant to investors’ beliefs about firm market value. Firms’ “abnormal” returns relative to a benchmark asset pricing model during such events summarize these changes expectations.<sup>3</sup> Here, we demonstrate that plausibly exogenous changes in the daily information set regarding the epidemic’s trajectory are correlated with firms’ stock returns.<sup>4</sup>

Third, our paper contributes to the very large literature in public health which attempts to explain the trajectory of infections during a pandemic.<sup>5</sup> In contrast to that research, we link changes in the estimated parameters and predictions of these models in real time to economic outcomes. To reiterate, we do not claim that the evolution of a pandemic must follow a purely exponential or logistic growth path. Rather, we explore whether the predictions of these models are informative of economic conditions, as manifest in their correlation with the market.<sup>6</sup> An interesting question for further research is the extent to which feedback from the predicted health and economic consequences of the outbreak affects future infections. For example, dire enough anticipated economic consequences might influence the set of policies used to combat the outbreak, thereby altering its trajectory ([Lucas, 1976](#)).

Finally, this paper relates to a rapidly emerging literature studying the economic consequences of COVID-19, and a more established literature investigating earlier pandemics. [Barro et al. \(2020\)](#), for example, argue that the decline in output during the 1918 to 1920 “Spanish Flu” epidemic provide a plausible mode of the economic consequences of COVID-19. Our analysis complements ([Ramelli and Wagner, 2020](#)), who focus on debt and international supply chains as key channels of exposure to the COVID-19 epidemic, and [Gormsen and Koijen \(2020\)](#), who use the performance of US futures’ markets during the outbreak to infer bounds on future GDP growth. Analyzing newspaper articles since 1900, [Baker et al. \(2002\)](#) find that the COVID-19 pandemic is the first infectious disease outbreak whose mention in the press is associated with a large daily market movement.

This paper proceeds as follows. Section 2 provides a brief description of infectious disease models and how investors might link the predictions of these models and to asset prices. Sections 3 and 4 apply our framework to COVID-19 and SARS. Section 5 concludes.

---

<sup>3</sup>[Wang et al. \(2013\)](#), for example, examines how the stocks of Taiwanese biotechnology companies respond to a series of infectious disease outbreaks.

<sup>4</sup>[Greenland et al. \(2019\)](#) exploit a change in US trade policy to identify firms’ exposure to greater import competition from China.

<sup>5</sup>Early contributions to this literature include [Ross \(1911\)](#), [Kermack and McKendrick \(1927\)](#), [Kermack and McKendrick \(1937\)](#) and [Richards \(1959\)](#).

<sup>6</sup>For an interesting discussion on the complexities associated with modeling an outbreak in real time, see <https://fivethirtyeight.com/features/why-its-so-freaking-hard-to-make-a-good-covid-19-model/>.

## 2 Modeling

In this section we outline how infectious disease outbreaks can be modeled in real time, and how investors might make use of the model’s estimated parameters.

### 2.1 Simple Models of Infectious Diseases

Exponential and logistic growth models are frequently used in biology and epidemiology to model infection and mortality. An exponential model,

$$C_t = ae^{(rt)} \quad (1)$$

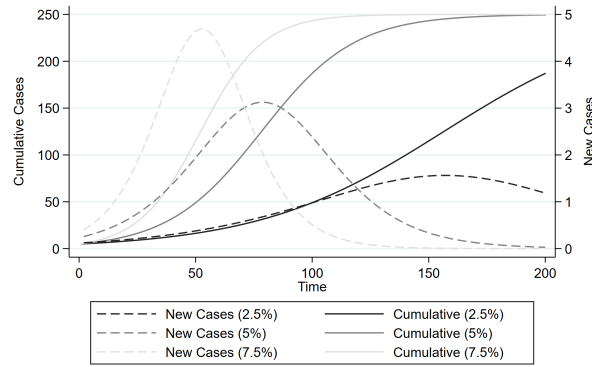
predicts the cumulative number of cases on day  $t$ ,  $C_t$ , as a function of the growth rate of infections in that country,  $r$ , the initial number of infected persons  $a$ , and time. In an exponential model, the number of infections per day continues to climb indefinitely. While clearly unrealistic ex-post, the exponential growth model is consistent with early stage pandemic growth rates.

In a logistic model (Richards, 1959), by contrast, the growth in infections grows exponentially initially, but then declines as the stock of infections approaches the population’s “carrying-capacity,” i.e., the cumulative number of people that ultimately will be infected. Carrying capacity is generally less than the full population. The cumulative number of infections on day  $t$  is given by

$$C_t = \frac{k}{1 + ce^{(-rt)}}, \quad (2)$$

where  $k$  is the carrying,  $c$  is a shift parameter (characterizing the number of initially infected persons) and  $r$  is the growth rate. Figure 1 provides an example of logistic infections for three different growth rates (2.5, 5 and 7.5 percent) assuming  $k = 250$  and  $c = 50$ . For each growth rate, we plot both the number of new cases each day (right axis) and the cumulative number of cases up to each day (left axis). As indicated in the figure, higher growth rates both shorten the time required to reach carrying capacity and increase the peak number of infections.

**Figure 1:** New and Cumulative New Cases Under the Logistic Model



Source: Authors’ calculations. Figure compares new and cumulative infections from days 1 to 200 assuming a logistic model with  $k = 250$  and  $c = 50$  and noted growth rates ( $r$ ).

Given data on the actual evolution of infections, the two parameters in equation 1 and the three parameters in equation 2 can be updated each day using the sequence of infections up to that

date. We estimate these sequences using STATA’s nonlinear least squares command (`nl`).<sup>7</sup> This command requires a vector of starting values, one for each parameter to be estimated.

We encounter two problems during our estimation of logistic functions in our applications below. First, estimates for each day  $t$  are sensitive to the choice of starting values for that day, particularly in the initial days of the pandemic. This feature of the estimation is not surprising: when the number of cases is relatively small, the data are consistent with a wide range of logistic curves, and the objective function across them may be relatively flat.

To increase the likelihood that our parameter estimates represent the *global* solution, we estimate 500 epidemiological models for each day, 250 for the logistic case, and 250 for the exponential case. In each iteration we use a different vector of starting values. For each day  $t$ , our first starting values are the estimated coefficients from the prior day, if available.<sup>8</sup> In the case of the logistic model, we then conduct a grid search defined by all triples  $\{r, c, k\}$  such that

$$\begin{aligned} r &\in \{0.01, 0.21, 0.41, 0.61, 0.81\} \\ c &\in \{\widehat{c^{t-1}}, 2 * \widehat{c^{t-1}}, 4 * \widehat{c^{t-1}}, \dots, 10 * \widehat{c^{t-1}}\} \\ k &\in \{\widehat{k^{t-1}}, 2 * \widehat{k^{t-1}}, 3 * \widehat{k^{t-1}}, \dots, 10 * \widehat{k^{t-1}}\} \end{aligned}$$

where hats over variables indicate prior estimates, and superscripts indicate the day on which they are estimated. If more than one of these initial starting values produces estimates, we choose the parameters from the model with the highest adjusted  $R^2$ . We estimate the exponential model similarly.

The second, more interesting, problem that we encounter during estimation of the logistic outbreak curves is that STATA’s `nl` routine may fail to converge. This failure generally occurs in the transition from relatively slow initial growth to subsequent, more obviously exponential growth as the pandemic proceeds. During this phase of the outbreak, the growth in the number of new cases each day is too large to fit a logistic function, i.e., the drop in the growth of new cases necessary to estimate a carrying capacity has not yet occurred.<sup>9</sup>

In our application below, we re-estimate both exponential and logistic parameters each day of an outbreak. To fix ideas, we simulate a 200-day cumulative logistic disease outbreak by generating a sequence of  $C_t = \frac{k}{1+ce^{(-rt)}} + |\epsilon_t|$  for  $t \in (1 : 200)$ , assuming  $k = 250$ ,  $r = .025$ ,  $c = 50$  and  $|\epsilon_t|$  is the absolute value of a draw from a standard normal distribution. For each day  $t$ , we estimate logistic and exponential parameters using the sequence of simulated infections up to that day.

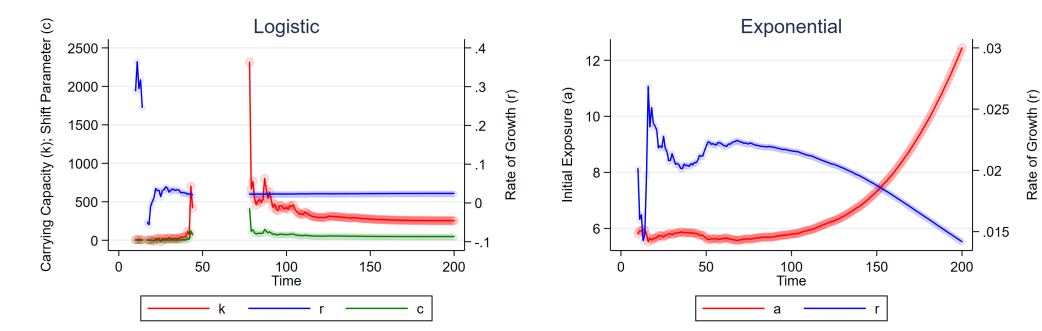
Figure 2 displays the results. Both sets of parameter estimates are volatile in the early stage of the outbreak. Logistic parameters are not available from days 47 through 78 due to lack on convergence, but settle down shortly thereafter, as the data increasingly conform to underlying logistic path. Exponential parameters are available for each day, but do not settle down as time goes on. The intuition for the unending increase in  $\hat{a}_t$  and decline in  $\hat{r}_t$  is as follows: because the simulated data are logistic, the only way to reconcile them with an exponential function is to have the estimate of initial exposure ( $\hat{a}_t$ ) rise as the estimate of the growth rate,  $\hat{r}_t$ , drops.

<sup>7</sup>We are exploring other estimation procedures for use in a future draft, including use of SIR and SEIR models, e.g., Li et al. (2020) and Atkeson (2020).

<sup>8</sup>If the prior day did not converge, we use the most recent prior day for which we have estimates.

<sup>9</sup>In a future draft we will consider an estimation strategy that nests these functions.

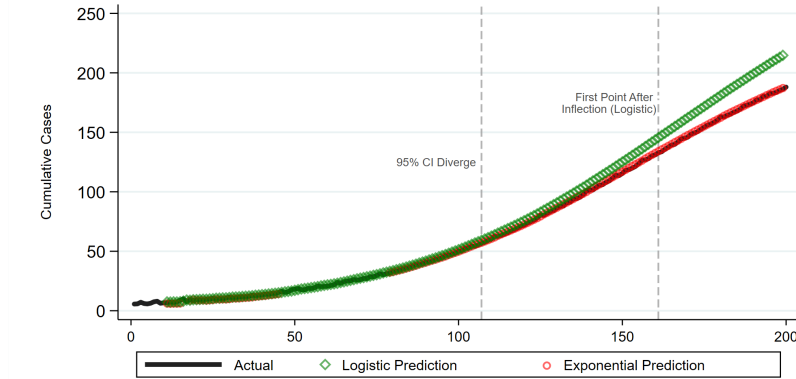
**Figure 2:** Parameter Estimates Using Simulated Logistic Pandemic



Source: authors' calculations. The left panel plots the sequence of logistic parameters,  $\hat{k}_t$ ,  $\hat{c}_t$  and  $\hat{r}_t$ , estimated using the information up to each day  $t$  on simulated data (see text). Right panel of Figure plots the analogous sequence of exponential parameters,  $\hat{a}_t$  and  $\hat{r}_t$ , using the same data. Missing estimates indicate lack of convergence (see text). Circles represent estimates. Solid lines connect estimates.

Figure 3 compares predicted cumulative cases for each model for each day  $t$  using the parameter estimates from day  $t - 1$ . We denote these predictions  $\widehat{C}_t^{t-1}$ , where the superscript  $t - 1$  refers to the timing of the information used to make the prediction, and the subscript refers to the day being predicted. As illustrated in the figure, predictions for the two models line up reasonably well during the initial phase of the pandemic. Their 95 percent confidence intervals (not shown) cease overlapping on  $t = 104$ . After this point, the exponential model continues to project an ever-increasing number of infections, while the logistic model's predictions head towards the “true” carrying capacity of 250.

**Figure 3:** Simulated Pandemic Daily Predictions ( $\widehat{C}_t^{t-1}$ )



Source: authors' calculations. Figure compares simulated “actual” cumulative infections to predicted infections ( $\widehat{C}_t^{t-1}$ ) under the logistic and exponential models. The prediction for each day  $t$  is based on the information available up to day  $t - 1$ . The two vertical lines in the figure note when the 95 percent confidence intervals of the two models' predictions (not shown) initially diverge, and when the logistic model's estimates first indicate that its inflection point has passed.

## 2.2 Modeling Economic Impact

Predicted cumulative cases for day  $t$  based on day  $t - 1$  information,  $\widehat{C}_t^{t-1}$ , can be compared to the day  $t$  forecast made with day  $t - 2$  information,  $\widehat{C}_t^{t-2}$ . The log difference in these predictions,

$$\Delta \ln \left( \widehat{C}_t^{-2,-1} \right) = \ln \left( \widehat{C}_t^{t-1} \right) - \ln \left( \widehat{C}_t^{t-2} \right), \quad (3)$$

captures *unexpected* changes in severity of the outbreak between these two days.<sup>10</sup> This potentially noisy “news” may be an important input into investors’ assessment of the economic impact of a pandemic. For example, a jump in estimated carrying capacity suggests a larger ultimate supply shock in terms of lost labor supply, while an uptick in the estimated growth rate has implications for healthcare capacity constraints.<sup>11</sup>

In our application below, we compare aggregate equity returns on day  $t$  to the difference in forecasts for that day using an OLS regression,

$$\Delta \ln (Index_t) = \alpha + \gamma_1 * \Delta \ln \left( \widehat{C}_t^{-2,-1} \right) + \gamma_2 X_t + \epsilon_t. \quad (4)$$

where  $\Delta \ln (Index_t)$  is the daily log change in either opening-to-opening or closing-to-closing prices in the aggregate market index of country  $i$ , and  $X_t$  represents a vector of country controls, e.g., changes in policy.<sup>12</sup>

We assess *firm  $j$* ’s sensitivity to the pandemic via an analogous specification,

$$R_{jt} = \delta + \beta_j^{C^{-2,-1}} * \Delta \ln \left( \widehat{C}_t^{-2,-1} \right) + \beta_j^{MKT} * \Delta \ln (Index_t) + \epsilon_t, \quad (5)$$

where the dependent variable is the daily return of firm  $j$  on day  $t$ . The second term on the right hand side accounts for the possibility that COVID-19 is no different than any other aggregate shock, and that a firm’s return during the pandemic merely reflects its more general co-movement with the market (Sharpe, 1964b). In our baseline assessment of firms’ exposure to the pandemic, we do not include this second covariate. When it is included,  $\beta_j^{C^{-2,-1}}$  represents the firm’s return in excess of its covariance with the market.

## 3 Application to COVID-19

In this section we provide real-time estimates of the outbreak parameters and infection predictions for COVID-19 in the United States. We then examine the relationship between changes in these predictions and both aggregate and firm-level returns in the United States.

<sup>10</sup>Timing is as follows. The number of infections on day  $t - 1$  is observed after the market closes on that day but before the market opens on day  $t$ . This day  $t - 1$  information is used to predict the number of cases for day  $t$ ,  $\widehat{C}_t^{t-1}$ , which is compared to  $\widehat{C}_t^{t-2}$ .

<sup>11</sup>As noted in the introduction, the evolution of these parameters may also trigger policy “events” either directly or as a result of their economic consequences, which may alter the underlying parameters of the outbreak. We do not currently account for such feedback, but plan to do so in a future draft.

<sup>12</sup>We are currently exploring more flexible specifications, e.g., those which might capture the switch between exponential and logistic models, as well as those which reveal any over- or undershooting of reactions.

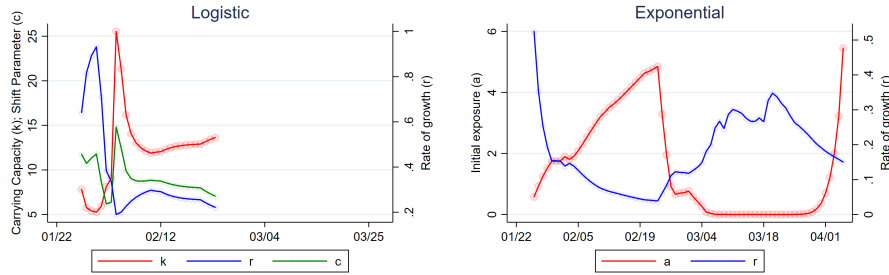


### 3.1 Epidemiological Model Parameters

Data on the cumulative number of COVID-19 cases in the United States as of each day are from the Johns Hopkins Coronavirus Resource Center.<sup>13</sup> The first COVID-19 case appeared in China in November of 2019, while the first cases in the United States and Italy appeared on January 20, 2020. Our analysis begins on January 22, 2020, the first day that the World Health Organization began issuing situation reports detailing new case emergence internationally. Appendix Figure A.1 displays the cumulative reported infections in the United States from January 22 through April 3, 2020.

We estimate logistic and exponential parameters (equations 1 and 2) for the United States by day as discussed in Section 2.1. The daily parameter estimates for the logistic estimation,  $\hat{k}_t$ ,  $\hat{c}_t$  and  $\hat{r}_t$  are displayed the left panel of Figure 4, while those for the exponential model,  $\hat{a}_t$  and  $\hat{r}_t$ , are reported in the right panel. Gaps in the time series in either figure represent lack of convergence.

**Figure 4:** Parameter Estimates for COVID-19



Source: Johns Hopkins Coronavirus Resource Center and authors' calculations. The left panel plots the sequence of logistic parameters,  $\hat{k}_{i_t}$ ,  $\hat{c}_{i_t}$  and  $\hat{r}_{i_t}$ , estimated using the cumulative infections in the US up to each day  $t$ . Right panel plots the analogous sequence of exponential parameters,  $\hat{a}_{i_t}$  and  $\hat{r}_{i_t}$ , using the same data. Missing estimates indicate lack of convergence (see text). Circles represent estimates. Solid lines connect estimates. Data currently extend to Friday March 27, 2020.

Logistic parameter estimates for the United States fail to converge after February 23, when the number of cases jumps abruptly from 15 to 51. That no parameter estimates are available after this date suggests that growth in new cases observed thus far is inconsistent with a leveling off, or carrying capacity, at least according to our estimation method. The exponential model, by contrast, converges for all days. As a result, we focus on the exponential model for the remainder of our analysis.

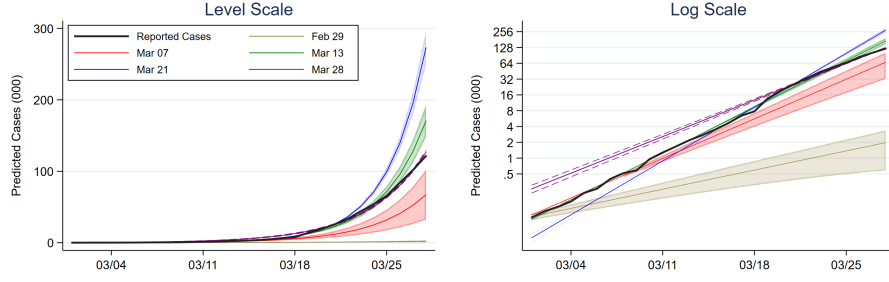
As the sharp changes in US exponential model parameters suggest, predicted cumulative infections vary substantially depending upon the day in which the underlying parameters are estimated. Figure 5 highlights this variability by comparing predicted cumulative infections based on the information available as of February 29 and March 7, 13, 21 and 28. The left panel displays these projections in levels, while the right panel uses a log scale. The five colored lines in the figure trace out each set of predictions. Dashed lines highlight 95 percent confidence intervals around these predictions. Finally, the confidence intervals are shaded for all days following the day upon which the prediction is based. To promote readability, we restrict the figure to the period after February 29. The black, solid line in the figure represents actual reported cases.

Predicted cumulative infections based on information as of February 29 are strikingly lower than predictions based on information as of March 21 due to the jump in reported cases between

<sup>13</sup>These data can be downloaded from <https://github.com/CSSEGISandData/COVID-19> and visualized at <https://coronavirus.jhu.edu/map.html>.



**Figure 5:** Predicted Cumulative Cases Using Different Days' Estimates (COVID-19)

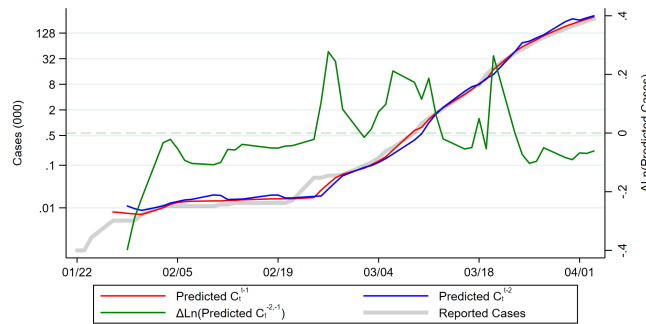


Source: Johns Hopkins Coronavirus Resource Center and authors' calculations. Figure displays predicted cases for the United States from March 18 onwards using the cumulative reported cases as of five dates: February 29, March 7, March 13, March 21 and March 28. Dashed lines represent 95 percent confidence intervals. Confidence intervals are shaded for all days after the information upon which the predictions are based.

those days. Indeed, according to the parameter estimates from March 21, US cases would number close to 300 thousand by the end of March. Equally striking is the downward shift in predicted cumulative cases that occurs between March 21 and March 28. It is precisely these kinds of changes in predicted cumulative cases that our analysis seeks to exploit.

Figure 6 uses the logistic parameter estimates in Figure 4 to plot  $\widehat{C}_t^{t-1}$  and  $\widehat{C}_t^{t-2}$  for the exponential model, i.e., the predicted number of cases on day  $t$  using the information up to day  $t-1$  and day  $t-2$ . Magnitudes for these cumulative cases are reported on the left axis. The right axis reports  $\Delta(\widehat{C}_t^{t-2,-1})$ , the log difference in these two predictions. Intuitively,  $\widehat{C}_t^{t-1}$  and  $\widehat{C}_t^{t-2}$  for the most part track each other closely. The former rises above the latter on days when reported cases jump, while the reverse happens when new cases are relatively flat.

**Figure 6:** Daily Logistic Predictions ( $\widehat{C}_t^{t-1}$  and  $\Delta \ln(\widehat{C}_t^{t-2,-1})$ ) for COVID-19



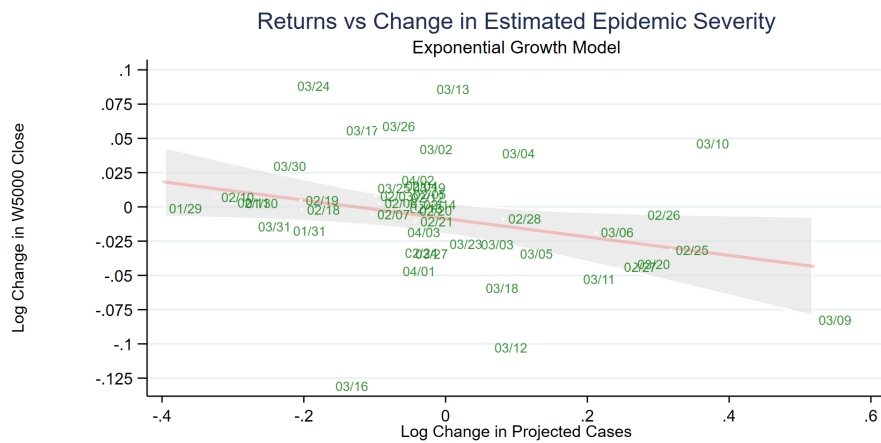
Source: Source: Johns Hopkins Coronavirus Resource Center and authors' calculations. Left axis reports the predicted cumulative cases for day  $t$  using information as of day  $t-1$ ,  $\widehat{C}_t^{t-1}$ , and day  $t-2$ ,  $\widehat{C}_t^{t-2}$ , under the exponential model. Right axis reports the log change in these two predictions,  $\Delta \ln(\widehat{C}_t^{t-2,-1})$ . Data currently extend to Friday April 3, 2020.

### 3.2 Aggregate US Returns During COVID-19

We examine the link between changes in model predictions and aggregate US stock via the Wilshire 5000 index.<sup>14</sup> We choose this index for its breadth, but note that results are qualitatively similar for other US market indexes.

Figure 7 plots the daily log change in the Wilshire 5000 index against unanticipated increases in cases,  $\Delta \ln(\widehat{C_t^{-2,-1}})$ . Their negative relationship indicates that returns are higher when the difference in predictions is lower, and *vice versa*. In particular, the approximate 20 percent decline in predicted cases that occurs on March 24 coincides with a greater than 9 percent growth in the market index.

**Figure 7:** Change in Predicted COVID-19 Cases ( $\widehat{\Delta C_t^{-2,-1}}$ ) vs Aggregate Market Returns



Source: Johns Hopkins Coronavirus Resource Center, Yahoo Finance and authors' calculations. Figure displays the daily log change in the Wilshire 5000 index against the log change in predicted cases under the exponential model for day  $t$  based on day  $t - 1$  and day  $t - 2$  information. Sample period is January 22 to April 3, 2020.

We investigate the relationship displayed in Figure 7 formally by estimating equation 4 via OLS. For each day, we compute  $\Delta \ln(Index_t)$  as the daily log change in either the closing or opening values of the Wilshire 5000. The estimation period consists of 47 trading days from January 22 to April 3.<sup>15</sup> The unit of observation is one day.

Coefficient estimates as well as robust standard errors are reported in Tables 1 and 2, where the former focuses on the daily opening-to-opening return and the latter on the daily closing-to-closing return. Coefficient estimates in the first column of each table indicate that a doubling of predicted cases using information from day  $t - 1$  versus day  $t - 2$  leads to average declines of -7.0 and -3.8 percent for closing and opening prices respectively. These effects are statistically significant at conventional levels.

In the second and subsequent columns of each table, we adjust the dependent and independent variables by the number of days since the last trading day. This adjustment insures that changes which transpire across weekends and holidays, when markets are closed, are not spuriously large compared to those that take place across successive calendar days. As indicated in the second column of each table, relationships remain statistically significant at conventional levels and now

<sup>14</sup>Data for the Wilshire 5000 are downloaded from Yahoo Finance.

<sup>15</sup>The actual number of trading days between these two dates is 50. We lose 3 days due to lack of estimates in the initial days of the outbreak.

**Table 1:** Changes in Predicted COVID-19 Cases ( $\widehat{\Delta C_t^{-1,-2}}$ ) vs Market Open Returns

	(1) $\Delta \text{Ln}(\text{Open})$	(2) $\Delta \text{Ln}(\text{Open})$	(3) $\Delta \text{Ln}(\text{Open})$	(4) $\Delta \text{Ln}(\text{Open})$	(5) $\Delta \text{Ln}(\text{Open})$	(6) $\Delta \text{Ln}(\text{Open})$
$\Delta \text{Ln}(\widehat{C^{-2,-1}})$	-0.040*** (0.013)	-0.049** (0.024)	-0.061** (0.024)	-0.063** (0.025)	-0.085** (0.033)	-0.055** (0.025)
$\Delta \text{Ln}(C^{-2,-1})$			0.019 (0.028)	0.026 (0.026)	0.028 (0.026)	0.006 (0.033)
$I(\Delta S \text{Index})$				-0.014 (0.014)		
$\Delta \text{Ln}(S \text{Index})$					-0.055 (0.061)	
Fiscal Stimulus						0.017 (0.013)
Constant	-0.007* (0.004)	-0.005 (0.004)	-0.008** (0.004)	-0.007* (0.004)	-0.006 (0.004)	-0.008* (0.004)
Observations	47	47	47	47	43	47
$R^2$	0.084	0.069	0.078	0.121	0.144	0.118
Daily Adjustment	N	Y	Y	Y	Y	Y

Source: Johns Hopkins Coronavirus Resource Center and authors' calculations.  $\Delta \text{Ln}(\text{Open}_t)$  and  $\Delta \text{Ln}(\text{Close}_t)$  are the daily log changes in the opening (i.e., day  $t - 1$  to day  $t$  open) and closing values of the Wilshire 5000.  $\Delta \text{Ln}(\widehat{C_t^{-2,-1}})$  is the change in predicted cases.  $\Delta \text{Ln}(C_t^{-2,-1})$  is the change in actual observed cases between days  $t - 2$  and  $t - 1$ .  $\Delta \text{Ln}(C_t^{-1,0})$  is the change in actual observed cases between days  $t - 1$  and  $t$ . Robust standard errors in parenthesis. Columns 2-6 divide all variables by the number of days since the last observation (i.e. over weekends). Sample period is January 22 to April 3, 2020.

have the interpretation of daily growth rates. Here, a doubling of predicted cases per day leads to average declines of 8.6 percent for closing and 4.8 percent for opening prices.

In column 3 of each table, we examine whether the explanatory power of  $\widehat{\Delta C_t^{-2,-1}}$  remains after controlling for a simple, local proxy of outbreak severity, the most recent change in reported cases. We use a slightly different variable in each table to account for the timing of the opening and closing returns. For the opening price regressions, we use  $\Delta \text{Ln}(C^{-2,-1})$  under the assumption that the only information available to predict the opening price on day  $t$  is the difference in reported cases from days  $t - 2$  and  $t - 1$ . For the closing price regressions, however, we use  $\Delta \text{Ln}(C^{-1,0})$  to informally allow for the possibility that, although day  $t$  cases are not officially available until after closing, some information might “leak out” during day  $t$  trading.

In both cases, these measures are positive but not statistically significant at conventional levels. Moreover, they have little impact on our coefficients of interest. These results suggest that the primary role local increases in reported cases play in determining market value is through their contribution to the overall sequence of reported infections, manifest in the estimated model parameters.

In the final three columns of Tables 1 and 2 we examine the robustness of our results to including coarse controls for policy. As the COVID-19 pandemic has unfolded in the United States, state and local governments as well as the federal government have undertaken various measures to control its spread and limit the economic burden the disease itself imposes. Enactment of such policies is by definition correlated with the severity of the outbreak, and some of them may be designed to stabilize equity markets, confounding our results.

**Table 2:** Change in Predicted COVID-19 Cases ( $\widehat{\Delta C_t^{-2,-1}}$ ) vs Market Close Returns

	(1) $\Delta \text{Ln}(\text{Close})$	(2) $\Delta \text{Ln}(\text{Close})$	(3) $\Delta \text{Ln}(\text{Close})$	(4) $\Delta \text{Ln}(\text{Close})$	(5) $\Delta \text{Ln}(\text{Close})$	(6) $\Delta \text{Ln}(\text{Close})$
$\Delta \text{Ln}(\widehat{C_t^{-2,-1}})$	-0.067** (0.030)	-0.080** (0.030)	-0.089*** (0.031)	-0.093*** (0.034)	-0.146*** (0.041)	-0.089*** (0.032)
$\Delta \text{Ln}(C_t^{-1,-0})$			0.033 (0.031)	0.055 (0.037)	0.065* (0.035)	0.034 (0.032)
$I(\Delta S \text{Index})$				-0.021 (0.018)		
$\Delta \text{Ln}(S \text{Index})$					-0.091 (0.076)	
Fiscal Stimulus						-0.005 (0.018)
Constant	-0.009 (0.006)	-0.005 (0.005)	-0.010** (0.004)	-0.010** (0.004)	-0.010** (0.004)	-0.010** (0.004)
Observations	47	47	47	47	43	47
$R^2$	0.092	0.086	0.103	0.145	0.224	0.104
Daily Adjustment	N	Y	Y	Y	Y	Y

Source: Johns Hopkins Coronavirus Resource Center and authors' calculations.  $\Delta \text{Ln}(\text{Open}_t)$  and  $\Delta \text{Ln}(\text{Close}_t)$  are the daily log changes in the opening (i.e., day  $t - 1$  to day  $t$  open) and closing values of the Wilshire 5000.  $\Delta \text{Ln}(\widehat{C_t^{-2,-1}})$  is the change in predicted cases for day  $t$  using information from days  $t - 1$  and  $t - 2$ .  $\Delta \text{Ln}(C_t^{-2,-1})$  is the change in actual observed cases between days  $t - 2$  and  $t - 1$ .  $\Delta \text{Ln}(C_t^{-1,0})$  is the change in actual observed cases between days  $t - 1$  and  $t$ . Robust standard errors in parenthesis. Columns 2-6 divide all variables by the number of days since the last observation (i.e. over weekends). Sample period is January 22 to April 3, 2020.

We consider two controls for policy. The first is a country-level index developed at Oxford University, the Government Response Stringency Index (SIndex), which tracks travel restrictions, trade patterns, school openings, social distancing and other such measures, by country and day.<sup>16</sup> We make use of this index in two ways in columns 4 and 5 of Tables 1 and 2. First, we include an indicator function  $I\{\Delta S \text{Index}\}$  which takes a value equal to one if the index changes on day  $t$ . Second, we use log changes in the index itself,  $\Delta \text{Ln}(S \text{Index})$ . As indicated in the tables, neither covariate is statistically significant at conventional levels, and their inclusion has little impact on the coefficient of interest.

Our second control for policy is a coarse measure of fiscal stimulus. This dummy variable is set to one for four days (chosen by the authors) upon which major fiscal policies were enacted. The ‘‘Coronavirus Preparedness and Response Supplemental Appropriations Act, 2020’’, which appropriated 8.3 billion dollars for preparations for the COVID-19 outbreak, was signed into law on March 6. Then, from March 25 to March 27, Congress voted for and the President signed into law the 2 trillion dollar ‘‘Coronavirus Aid, Relief, and Economic Security Act.’’ As reported in the table, this dummy variable, too, is statistically insignificant at conventional levels, and exerts no influence on the coefficient of interest.

Policy variables' lack of statistical significance is somewhat puzzling. One explanation for this outcome is that these measures are a function of the information contained in the cumulative reported cases, and therefore retain no independent explanatory power. On the other hand, the various government policies included in the SIndex may have offsetting effects. For example, while

<sup>16</sup>This index can be downloaded from <https://www.bsg.ox.ac.uk/research/research-projects/oxford-covid-19-government-response-tracker>.

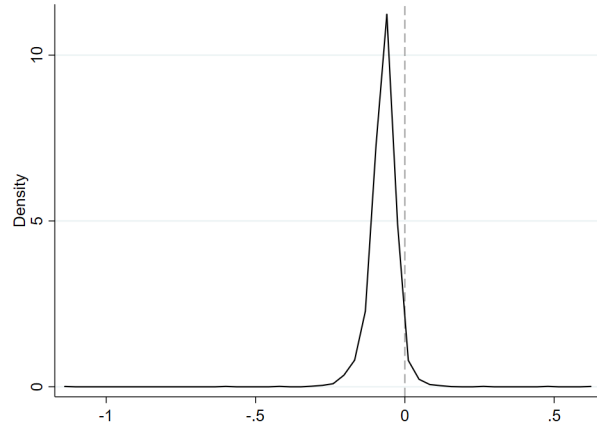
social distancing measures might be interpreted by the market as a force that reduces the economic severity of the crisis, they may also be taken as a signal that the crisis is worse than publicly available data suggest. At present, we do not have the degrees of freedom to explore the impact of individual elements of the this index, but plan to do so in a future draft when inclusion of additional countries in the analysis allows for panel estimation.

### 3.3 Firm-Level US Returns During COVID-19

In this section we examine the relationship between unanticipated changes in predictions and returns at the firm level. The sample period is January 22 to April 3, 2020. Data are taken from Bloomberg and Yahoo finance.<sup>17</sup> We link firms to balance sheet information in Compustat via their CUSIP numbers. In the analysis that follows, we focus on the sample of 4070 firms incorporated in the United States for which we observe returns. These firms span 505 six-digit NAICS classifications and 249 4-digit NAICS classifications.

As a baseline, we assess firms' exposure to COVID-19 by estimating equation 5 *omitting* the market term  $\Delta \ln(Index_t)$ . We estimate this regression separately for each firm  $j$ , yielding 4070  $\widehat{\beta}_j^{C^{-2,-1}}$ . The distribution of these exposures is summarized by the kernel density reported in Figure 8. Intuitively, given the behavior of the overall market discussed in the above, we find that the overwhelming majority of firm-level sensitivities are below zero, indicating that the firms' returns generally have a negative relationship with predicted increases in cumulative infections,  $\Delta \ln(\widehat{C}_t^{-2,-1})$ .

**Figure 8:** Distribution of US Firms' Sensitivity to COVID-19:  $\widehat{\beta}_j^{C^{-2,-1}}$



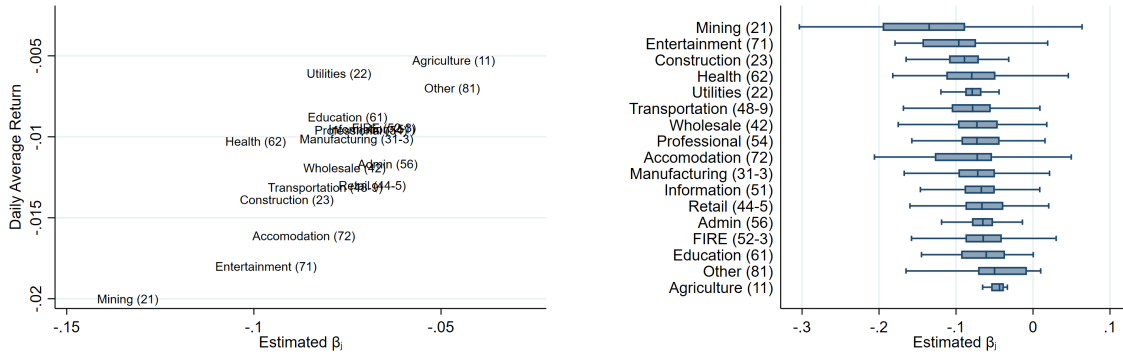
Source: Johns Hopkins Coronavirus Resource Center, Bloomberg, Yahoo Finance and authors' calculations. Figure reports the distribution of firm sensitivities ( $\widehat{\beta}_j^{C^{-2,-1}}$ ) to unanticipated changes in exponential model predictions,  $\Delta \widehat{C}_t^{-2,-1}$ , estimated using equation 5. Sample period is January 22 to April 3, 2020.

<sup>17</sup>We use Yahoo for stock prices after March 18, the last day for which we had access to Bloomberg terminals. We use the Bloomberg data to filter our Yahoo sample as follows. We match firms by ticker from January, 22 to March 18. If returns from the two sources differ by 0.01 on more than one day, or if they differ by more than 1 on any day, we deem that firm's returns unreliable and drop them from the analysis. The remaining returns have an in-sample correlation of 99.6 percent during the overlap period.

The right panel of Figure 9 summarizes firms' exposure to COVID-19 by two-digit NAICS sector. While sectors clearly vary in (and are sorted by) their median level of exposure, there is substantial variation across firms within sectors. The left panel of the figure plots firms' average exposure by sector against their average daily returns between January 17, the last trading day prior to the United States' first case, and April 3. We compute a firm's mean daily return over this period,  $\bar{r}_j$ , where the bar denotes an average, as the geometric mean of its daily returns,  $R_{jt}$ , during the holding period.

The position of sectors in the figure is intuitive. Firms operating in sectors more heavily affected by the imposition of social distancing – Accommodations, Entertainment, and Transportation – exhibit negative values for  $\widehat{\beta}_j^{C-2,-1}$  and relatively large declines in daily average returns. The position of Mining, in the extreme lower left position of the figure, is also unsurprising given the sharp contraction in economic activity.<sup>18</sup> Agriculture, Utilities, Education, Professional Services and FIRE (Finance, Insurance and Real Estate) are towards the upper right of the figure. These sectors are less exposed to COVID-19 due to their necessity or their ability to conduct business online, and experience relatively less negative average returns.

**Figure 9:** US Firms' Sensitivity to COVID-19 ( $\widehat{\beta}_j^C$ ), by NAICS Sector



Source: Johns Hopkins Coronavirus Resource Center, Bloomberg, Yahoo Finance and authors' calculations. Figure reports the distribution of firm sensitivities ( $\widehat{\beta}_j^C$ ) to unanticipated changes in exponential model projections,  $\Delta C_t^{-2,-1}$ , estimated using equation 5. Geometric average of daily returns calculated from January 17 - April 3, 2020.

We examine the extent to which exposure to COVID-19 affects firms' *cumulative* change in firm value (thus far) using a cross-sectional OLS regression,

$$\bar{r}_j = \nu_1 \widehat{\beta}_j^C + \nu_2 \widehat{\beta}_j^{MKT} + \xi_j, \quad (6)$$

where  $\bar{r}_j$  is firm  $j$ 's average daily return from January 22 to April 3, and  $\widehat{\beta}_j^C$  and  $\widehat{\beta}_j^{MKT}$  are its sensitivities to the log changes in predicted cumulative infections and the US market index (Wilshire 5000) estimated from equation 5. To the extent that exposure to COVID-19 influences firm returns beyond their co-movement with the market, both terms in equation 6 will have explanatory power. This regression similar in spirit to those proposed by Fama and MacBeth (1973), though here we use a single cross section rather than repeated cross sections, i.e., one for each day as the crisis unfolds.<sup>19</sup>

<sup>18</sup>Returns in mining, which include oil and gas extraction, are also affected by recent disagreements within OPEC, which are potentially endogenous to the pandemic.

<sup>19</sup>Repeated cross-sectional regression more in line with Fama and MacBeth (1973) will be added in a future draft.

**Table 3:** Attributing Holding Period Returns to US COVID-19 Cases

	$\widehat{\bar{r}_j}$	$\bar{r}_j$
$\widehat{\beta_j^{C-2,-1}}$	0.050*** (0.008)	0.023*** (0.007)
$\widehat{\beta_j^{MKT}}$		-0.007*** (0.001)
Constant	-0.006*** (0.001)	-0.003*** (0.001)
Observations	4070	4070
$R^2$	0.114	0.198

Source: Johns Hopkins Coronavirus Resource Center, Bloomberg, Yahoo Finance and authors' calculations. Table reports results of cross-sectional OLS regression of firms' average return between January 22 and April 3,  $\bar{r}_j$ , on  $\widehat{\beta_j^C}$  and  $\widehat{\beta_j^{MKT}}$ , the coefficient estimates from equation 5. Robust standard errors reported in parenthesis below coefficients. The standard deviations of  $\bar{r}_j$ ,  $\widehat{\beta_j^C}$  and  $\widehat{\beta_j^{MKT}}$  are 0.008, 0.051 and 0.043.

Results are reported in Table 3, where the first column focuses on firms' sensitivity to COVID-19, and the second column includes both exposures. The coefficient estimate in column 1, 0.050, implies that a one standard deviation increase in  $\widehat{\beta_j^{C-2,-1}}$  is associated with a 0.33 standard deviation reduction in average return, a sizable influence.<sup>20</sup> The estimates in column 2 indicate that this influence remains even after accounting for firms' sensitivity to the market. Here, the magnitude of the coefficient, 0.023, implies that a one standard deviation increase in exposure to COVID-19 is associated with a 0.11 standard deviation decrease in returns, or roughly one quarter of the magnitude of the implied impact of a standard deviation change in market exposure.

## 4 Application to SARS

In this section we demonstrate historical precedent for the link between US stock market returns and COVID-19 discussed above by reporting a similar link during the Severe Acute Respiratory Syndrome (SARS) outbreak in Honk Kong nearly 20 year years earlier.

The first SARS case was identified in Foshan, China in November 2002, but was not recognized as such until much later. According to WHO (2006), on February 10, 2003 a member of the WHO in China received an email asking:

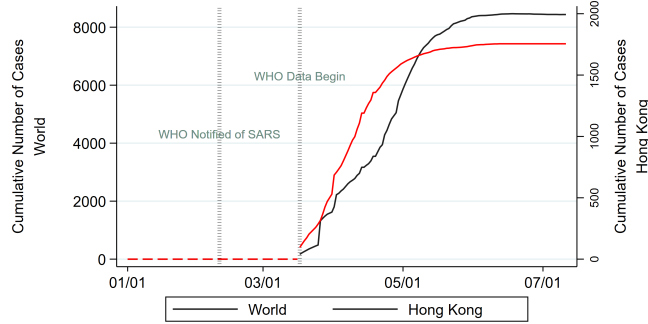
“Am wondering if you would have information on the strange contagious disease (similar to pneumonia with invalidating effect on lung) which has already left more than 100 people dead in ... Guangdong Province, in the space of 1 week. The outbreak is not allowed to be made known to the public via the media, but people are already aware of it (through hospital workers) and there is a ‘panic’ attitude.”

<sup>20</sup>The standard deviations of  $\bar{r}_j$ ,  $\widehat{\beta_j^C}$  and  $\widehat{\beta_j^{MKT}}$  are 0.008, 0.051 and 0.043.



The WHO immediately began an investigation into SARS, and started releasing regular reports of suspected and confirmed cases beginning March 17, 2003.<sup>21</sup> The World Health Organization (WHO) declared SARS contained in July 2003, though cases continued to be reported until May 2004. Figure 10 plots the cumulative number of confirmed SARS infections worldwide (left scale) and in Hong Kong (right scale). The two vertical lines in the figure note the days on which the WHO officially received the aforementioned email, and the first day on which the WHO began reporting the number of infections on each weekday.

**Figure 10: SARS Infections in Hong Kong and Worldwide During 2003**



Source: World Health Organization and authors' calculations. Figure displays the cumulative reported SARS infections in Hong Kong and the rest of the world from January 1, 2003 to July 11, 2003. The two vertical lines in the figure note the days on which the WHO officially received the aforementioned email, and the first day on which the WHO began reporting the number of infections on each weekday.

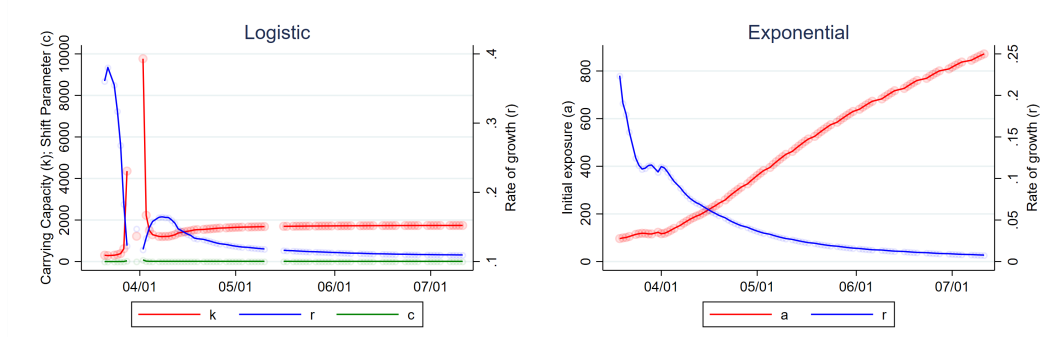
Hong Kong and China accounted for the vast majority of cases worldwide.<sup>22</sup> We focus our analysis on Hong Kong for two reasons related to data reliability. First, while China acknowledged having over 300 cases of “atypical pneumonia” in February, the Ministry of Health did not provide day-by-day counts until March 26. In fact, on March 17, the day before WHO began releasing daily situation reports, Chinese authorities informed the WHO that “[t]he outbreak in Guangdong is said to have tapered off.” The next day, cases were reported in 8 locations other than China – including Hong Kong. When China did begin reporting daily counts, on March 26, the first count was 800 cases. This large initial level of infections accounts for the sharp jump in world counts displayed for that day in Figure 10. Lack of real-time infection updates in mainland China prior to this jump undermines reliable estimation of model parameters, thereby impeding accurate assessment of unanticipated changes in infections. Second, it is unclear how China’s restrictions on foreign ownership of companies’ “A shares” during this period affects the extent to which such unanticipated changes will be reflected in Mainland firms’ equity value.

We estimate equations 1 and 2 by day for each country as discussed in Section 2. The daily parameter estimates for the logistic estimation,  $\hat{k}_t$ ,  $\hat{c}_t$  and  $\hat{r}_t$  are displayed graphically in the left panel of Figure 11. The right panel displays analogous estimates for the exponential function. Gaps in either panel’s time series represent lack of convergence. As indicated in the figure, logistic parameters fail to converge for several days early in the outbreak, and then once again when the estimates have started to settle down in the beginning of May. The exponential model, by contrast, converges on every day in the sample period.

<sup>21</sup>Counts were released every weekday. These data can be downloaded from <https://www.who.int/csr/sars/country/en/>. A timeline of WHO activities related to SARS events can be found at [https://www.who.int/csr/don/2003\\_07\\_04/en/](https://www.who.int/csr/don/2003_07_04/en/).

<sup>22</sup>Reported cases for China are plotted in appendix Figure A.2.

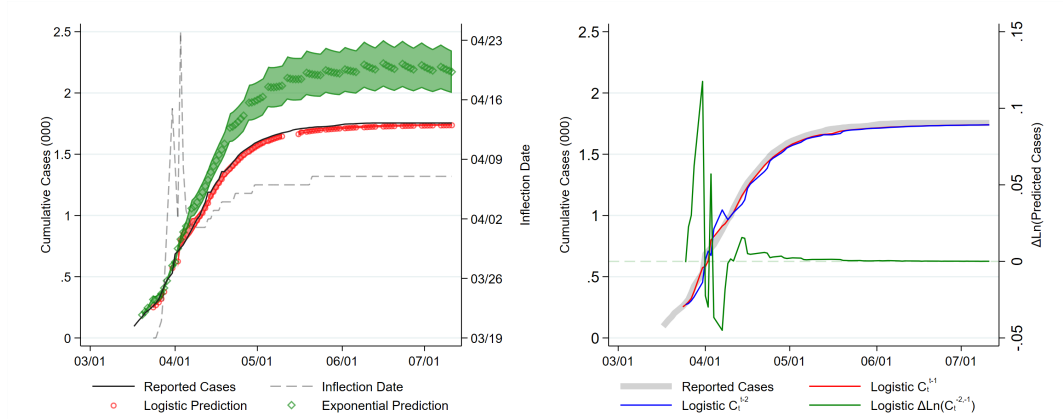
**Figure 11: Parameter Estimates for SARS**



Source: World Health Organization and authors' calculations. The left panel plots the sequence of logistic parameters,  $\hat{k}_t$ ,  $\hat{c}_t$  and  $\hat{r}_t$ , estimated using the information up to each day  $t$  on the cumulative reported cases for Hong Kong displayed in Figure 10. Right panel Figure plots the analogous sequence of exponential parameters,  $\hat{a}_{it}$  and  $\hat{r}_{it}$ , using the same data. Missing estimates indicate lack of convergence (see text). Circles represent estimates. Solid lines connect estimates.

In the left panel of Figure 12, we compare the predictions of the two models. In each case, parameter estimates from day  $t - 1$  are used to predict the cumulative number of cases for day  $t$ . Shading represents 95 percent confidence intervals. As indicated in the panel, predicted infections under the two models (left axis) are similar through the first week in April, but diverge thereafter. Interestingly, this divergence coincides with a stabilization of the estimated inflection point of the logistic curve (right axis), which, as illustrated by the dashed grey line in the panel, hovers between April 5 and 7 from April 5 onward.<sup>23</sup>

**Figure 12: Daily Predictions ( $\widehat{C}_t^{t-1}$ ) for SARS**



Source: World Health Organization and authors' calculations. Left panel displays predicted cumulative cases for each day  $t$ ,  $\widehat{C}_t^{t-1}$ , information as of day  $t - 1$ , based on parameter estimates reported in Figure 11. Shading spans 95 percent confidence intervals. Dashed line (right scale) traces out the estimated of the logistic curve's inflection point ( $\ln(\hat{c}_t)/\hat{r}_t$ ). Right panel reports day  $t$  predicted cumulative cases under the logistic model using information as of day  $t - 1$ ,  $\widehat{C}_t^{t-1}$ , and day  $t - 2$ ,  $\widehat{C}_t^{t-2}$ , as well as the log difference between these predictions,  $\Delta \ln(\widehat{C}_t^{t-2,t-1})$ . Missing estimates in left panel indicate lack of convergence (see text).

We use the predictions of the logistic model for the remainder of the analysis. The right panel

<sup>23</sup>The inflection point is given by  $\ln(\hat{c}_t)/\hat{r}_t$ .



**Table 4:** Changes in Predicted SARS Cases vs Hang Seng Index Returns

	(1) $\Delta \text{Ln}(\text{Close})$	(2) $\Delta \text{Ln}(\text{Close})$	(3) $\Delta \text{Ln}(\text{Close})$	(4) $\Delta \text{Ln}(\text{Close})$
$\Delta \text{Ln}(\widehat{C}^{-2,-1})$	-0.0752*** (0.0241)	-0.1095*** (0.0396)	-0.0891** (0.0427)	-0.0923* (0.0537)
$\Delta \text{Ln}(C^{-2,-1})$			-0.0445** (0.0200)	-0.0483 (0.0294)
Constant	0.0018 (0.0013)	0.0010 (0.0011)	0.0019* (0.0011)	0.0025 (0.0051)
Daily Adjustment	N	Y	Y	Y
Month FE	N	N	N	Y
Observations	70	70	70	70
$R^2$	0.108	0.060	0.103	0.111

Source: World Health Organization, Yahoo Finance and authors' calculations.  $\Delta \text{Ln}(\text{Close}_t)$  is the daily log change (i.e., day  $t - 1$  to day  $t$ ) closing values Hang Seng Index.  $\Delta \text{Ln}(\widehat{C}_t^{-2,-1})$  is the change in predicted cases for day  $t$  using information from days  $t - 1$  and  $t - 2$ .  $\Delta \text{Ln}(C_t^{-2,-1})$  is the change in reported cases between days  $t - 1$  and  $t$ . Robust standard errors in parenthesis. Columns 2-4 divide all variables by the number of days since the last observation (i.e. over weekends). Column 4 includes month fixed effects.

Across specifications, coefficient estimates indicate an average decline of 8 to 11 percent in response to a doubling of predicted cumulative infections.

## 5 Conclusion

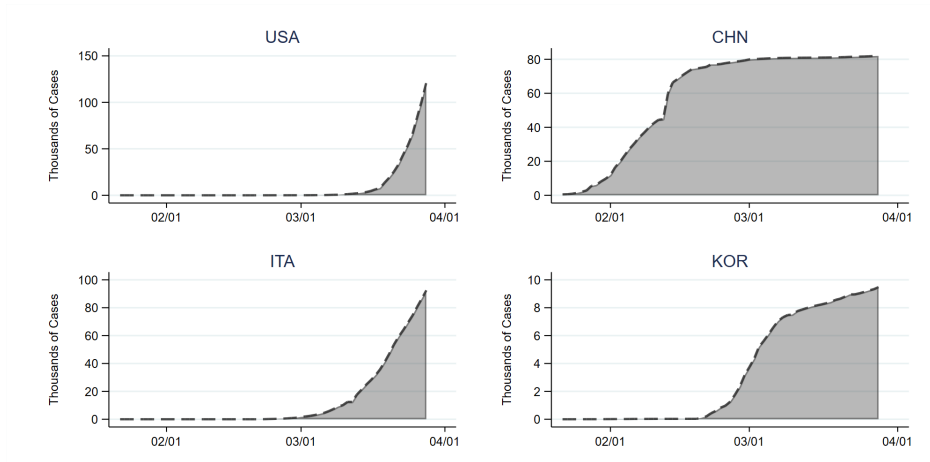
This paper shows that day-to-day changes in the predictions of standard models of infectious disease forecast changes in aggregate stock returns in Hong Kong during the SARS outbreak and the United States during the COVID-19 pandemic. In future updates to this paper, we plan to extend the analysis to other countries and pandemics, and to investigate the link between individual firms' returns and their exposure to public health crises via domestic and international input and output linkages as well as the demographics and occupations of their labor forces.

## References

- Atkeson, A. (2020, March). What will be the economic impact of covid-19 in the us? rough estimates of disease scenarios. Working Paper 26867, National Bureau of Economic Research.
- Baker, G., R. Gibbons, and K. J. Murphy (2002, February). Relational contracts and the theory of the firm. *The Quarterly Journal of Economics* 117(1), 39–84.
- Ball, R. and P. Brown (1968). An empirical evaluation of accounting income numbers. *Journal of accounting research*, 159–178.
- Barro, R. J., J. F. Ursua, and J. Weng (2020, March). The coronavirus and the great influenza pandemic: Lessons from the “spanish flu” for the coronavirus’s potential effects on mortality and economic activity. Working Paper 26866, National Bureau of Economic Research.
- Berger, D., K. Herkenhoff, and S. Mongey (2020). A seir infectious disease model with testing and conditional quarantine. *Working Paper*.
- Campbell, J. Y. and R. J. Shiller (1988). The dividend-price ratio and expectations of future dividends and discount factors. *The Review of Financial Studies* 1(3), 195–228.
- Fama, E. and J. D. MacBeth (1973). Risk, return, and equilibrium: Emprirical tests. *Journal of Political Economy*.
- Fama, E. F., L. Fisher, M. C. Jensen, and R. Roll (1969). The Adjustment of Stock Prices to New Information. *International Economic Review* 10.
- Fama, E. F. and K. R. French (1988). Dividend yields and expected stock returns. *Journal of financial economics* 22(1), 3–25.
- Gormsen, N. J. and R. S. Koijen (2020). Coronavirus: Impact on stock prices and growth expectations. *University of Chicago, Becker Friedman Institute for Economics Working Paper* (2020-22).
- Greenland, A., M. Ion, J. Lopresti, and P. K. Schott (2019). Using equity market reactions to infer exposure to trade liberalization. Technical report, Working Paper.
- Kermack, W. O. and A. G. McKendrick (1927). A contribution to the mathematical theory of epidemics. *Proceedings of the royal society of london. Series A, Containing papers of a mathematical and physical character* 115(772), 700–721.
- Kermack, W. O. and A. G. McKendrick (1937). Contributions to the mathematical theory of epidemics iv. analysis of experimental epidemics of the virus disease mouse ectromelia. *Journal of Hygiene* 37(2), 172–187.
- Keynes, J. M. (1937). The general theory of employment. *The quarterly journal of economics* 51(2), 209–223.
- Knight, F. H. (1921). Risk, uncertainty and profit. *Library of Economics and Liberty*.
- Li, R., S. Pei, B. Chen, Y. Song, T. Zhang, W. Yang, and J. Shaman (2020). Substantial undocumented infection facilitates the rapid dissemination of novel coronavirus (sars-cov2). *Science*.
- Lucas, R. E. (1976). Econometric policy evaluation: A critique. In *Carnegie-Rochester conference series on public policy*, Volume 1, pp. 19–46.

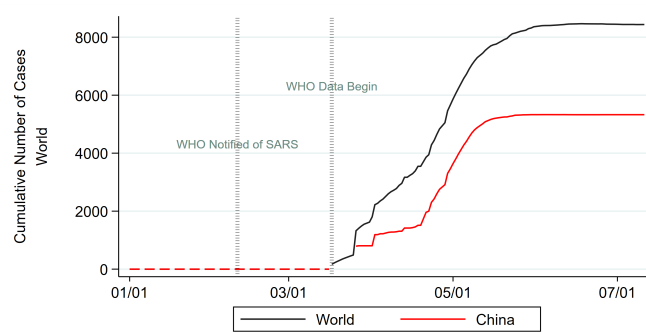
- Piguillem, F. and L. Shi (2020). The optimal covid-19 quarantine and testing policies. *Working Paper*.
- Ramelli, S. and A. F. Wagner (2020). Feverish stock price reactions to covid-19. *Swiss Finance Institute Research Paper* (20-12).
- Richards, F. J. (1959, 06). A Flexible Growth Function for Empirical Use. *Journal of Experimental Botany* 10(2), 290–301.
- Ross, R. (1911). *The Prevention of Malaria*. John Murray.
- Sharpe, W. F. (1964a). Capital Asset Prices: A Theory of Market Equilibrium Under Conditions of Risk.
- Sharpe, W. F. (1964b). Capital Asset Prices: A Theory of Market Equilibrium Under Conditions of Risk.
- Wang, Y.-H., F.-J. Yang, and L.-J. Chen (2013). An investor’s perspective on infectious diseases and their influence on market behavior. *Journal of Business Economics and Management* 14(sup1), S112–S127.
- WHO (2006). *SARS: how a global epidemic was stopped*. Manila: WHO Regional Office for the Western Pacific.

**Figure A.1: Actual COVID-19 Cases, By Country**



Source: Johns Hopkins Coronavirus Resource Center and authors' calculations. Figure displays the COVID-19 up to March 28.

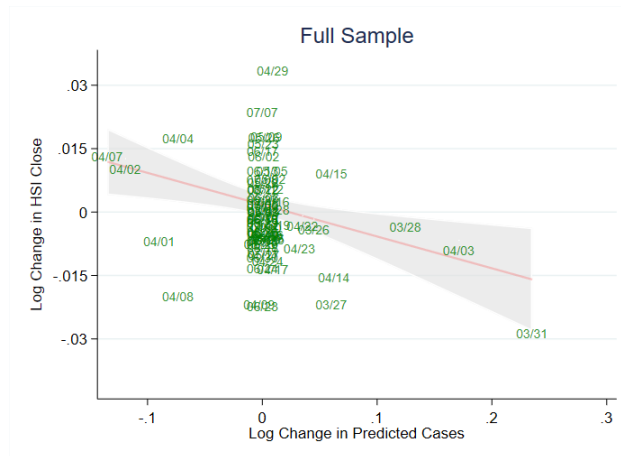
**Figure A.2: SARS Infections in China and Worldwide During 2003**



Source: World Health Organization and authors' calculations. Figure displays the cumulative reported SARS infections in China and the rest of the world from January 1, 2003 to July 11, 2003.



**Figure A.3:** Changes in Predicted SARS Cases vs HSI Index



Source: Johns Hopkins Coronavirus Resource Center, Yahoo Finance and authors' calculations. Figure displays the daily log change in the Hang Seng Index against the log change in projected cases for day  $t$  based on day  $t - 1$  and day  $t - 2$  information.